

Evaluating synthetic fuel production: A case study on the influence of electricity and CO₂ price variations

David Huber^{a,*}, Felix Birkelbach^a, René Hofmann^a

^aTU Wien, Institute of Energy Systems and Thermodynamics, Getreidemarkt 9/BA, 1060 Vienna, Austria

Abstract

To combat climate change, we need to reduce emissions from the transport sector. Synthetic fuels are a long-term solution for aviation, maritime and heavy machinery. Large-scale use requires cost-effectiveness, efficient production and resilience to price changes. In this case study, we simultaneously optimize the cell voltage of the solid oxide electrolysis cell, the heat exchanger network and the heat supply of a PtL-plant. PtL-efficiency and production costs are used as objectives to generate multiple Pareto fronts for future price scenarios. The results show that the sensitivity to price changes has different impacts on design and operating parameters, which can lead to unattractive solution domains in the Pareto front. Currently, synthetic fuels can be produced at 1.83–2.36 €/kg. In the best case, at 1.42–1.97 €/kg and 3.88–4.28 €/kg in the worst case. This paper supports decision-makers in planning PtL-plants to ensure sustainable synthetic fuel availability on a global scale.

Keywords: sustainable fuel production, synthetic fuels, power-to-liquid, optimization, electricity and CO₂ price changes

1. Introduction

The leading causes of anthropogenic climate change are CO₂ emissions from the combustion of fossil fuels. The transport sector contributed with 7.95 Gt to approx. 21.60 % of the annual CO₂ emissions in 2022 [1, 2]. Facing these figures, there is an increasing need to create a climate-neutral transport sector. Synthetic fuels from renewable energy sources and CO₂ offer a promising solution. They significantly reduce the carbon footprint from the transport sector since the combustion process only releases the CO₂ that was previously taken out of the atmosphere or has been emitted from another source, such as a cement plant [3]. Unlike fossil fuels, no previously bonded CO₂ is released into the atmosphere. Promising applications are conceivable both in the short term

for existing passenger cars and in the long term for non-electrifiable sectors such as shipping, aviation and heavy machinery.

Today's Power-to-liquid (PtL) plants already produce several thousand tons of methanol and Fischer-Tropsch (FT) fuels annually. A list of currently operating plants and upcoming projects is provided by Pratschner et al. [4]. There is also an interactive map with additional sites in [5]. Another interesting map is the Power-to-X potential atlas by Fraunhofer IEE [6], which illustrates the enormous potential of synthetic fuel production sites. So far, little is known about the production costs of the existing plants. The demonstration plant in Haru Oni, Chile, for example, produces fuel at costs of 50 €/L [7]. However, these costs are not representative for large-scale industrial production. They nevertheless reflect the problem of economically viable production. The production costs must be lowered to be financially relevant to end-users [8]. The analyses of Ueckerdt et al. [3] predict long-term produc-

*Corresponding author

Email address: david.huber@tuwien.ac.at (David Huber)

tion costs of less than 1 €/L. With production costs in the same order of magnitude as conventional fuels, synthetic fuels will be deployed.

The crucial challenges include producing fuels with competitive costs and in sufficient quantities. The production of synthetic fuels requires a complex interaction of processes, where various parameters, such as the operating point and heat integration, significantly impact costs and efficiency. Applying mathematical programming, the plant design, respectively, the interaction of sub-components can be optimized to meet defined objectives. However, optimizing only a constrained single objective problem may result in insufficient performance of other critical aspects compared to multi-criteria optimization (MOO) [9]. In this paper, the objectives PtL-efficiency and production costs are used.

The electricity price is another crucial factor that significantly impacts the production costs of synthetic fuels. Although production costs are not directly affected by CO₂ prices, the fuel price for end users is nevertheless affected. For the end users, the point at which the CO₂ prices are applied is not decisive since they are added to the fuel costs anyway. In this paper, we consider the CO₂ price as part of the production cost to ensure comparability with conventionally produced fuels. The prices for renewable electricity and CO₂ certificates can be subject to significant fluctuations due to technological leaps and changing policies. These fluctuations can have unforeseen effects on the economics of synthetic fuel costs. For the design optimization of the PtL-plant, defined assumptions must be made for electricity and CO₂ prices. Changing prices after the commissioning of the plant can have unwanted effects on production costs. During the planning phase, it is essential to analyze the effects of price changes and consider their consequences when choosing the optimal plant design and operation.

1.1. Novelty & Contribution

In this paper, we conduct a parametric study to understand the impact of changing electricity and CO₂ prices on the production costs of synthetic fuels. We perform an in-depth analysis based on the coupled optimization of the operating characteristics, the heat exchanger network (HEN) and the internal heat supply. PtL-efficiency and fuel production cost are used as objectives of the MOO problem. Starting from a Pareto front at current feedstock

prices, the CO₂ and electricity prices are varied. We examine each cost parameter's sensitivity to operating and design characteristics and derive projected Pareto fronts within reasonable price scenarios. We show that fluctuating cost parameters affect design and operation parameters differently. Accordingly, the relevant region of the Pareto front can be narrowed and the plant can be designed to be more resilient. Our analyses are crucial to assess fuel production costs to changing market conditions and policies. This allows us to ensure that synthetic fuels can be made economically viable and available in sufficient quantities to meet global demand.

1.2. Paper Organization

The novel 1 MW PtL-plant with its main components and characteristics is presented in Section 2.1. In Section 2.2, the methods for optimization, linearization and the transfer to MILP are presented. In Section 3.1 the modeling and the two antagonistic objectives, PtL-efficiency and production cost, are presented. Further, in Section 3.2 the correlation of the cost parameters with the objective functions and the parameter domain are described. In Section 4, the parameter study results and the cost parameters' sensitivities are analyzed and discussed.

2. Materials & Methods

2.1. System Description

In the context of the *IFE* (de.: Innovation Flüssige Energie, eng.: Innovation Liquid Energy) research project, a PtL-plant is designed to produce synthetic fuels using water, renewable electricity, exhaust gas from a cement plant and air as feedstock. The plant is designed with a maximum electrolysis capacity of approximately 1 MW using a high-temperature solid oxide co-electrolysis (co-SOEC). Figure 1 shows a schematic of the process. Notably, the schematic does not include valves, pumps, or compressors but indicates heat exchangers (HEX) for heat transfer. The cold process streams are shown in blue, and the hot process streams are shown in red.

The PtL process is divided into the following five main components. A more detailed description of the process can be found in [10, 11].

Steam Generation Pure water at 20 °C is preheated, evaporated, and superheated in the steam generator.

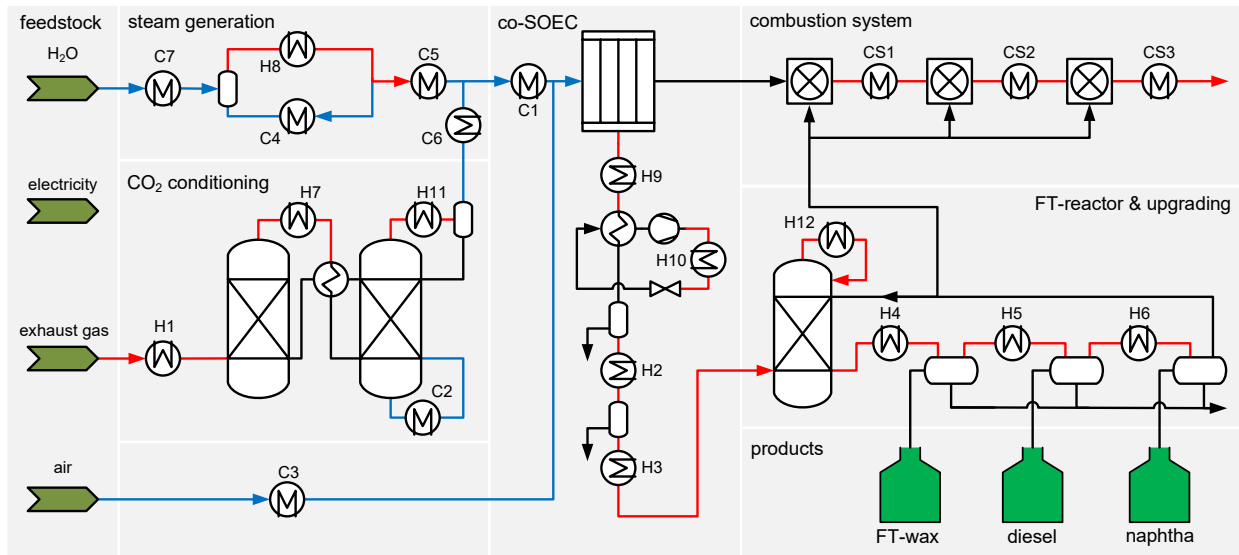


Figure 1: Schematic representation of the 1 MW PtL-plant with the five main components and the heat exchangers. Adapted from [10].

CO₂ Conditioning The PtL-process utilizes exhaust gas from a cement plant with 15.17 wt% CO₂, 81.11 wt% N₂, and 3.72 wt% H₂O at 40 °C. The CO₂ is conditioned to a purity of 98.73 wt% with low residual water content through adsorption and desorption processes.

co-SOEC The central component is the co-SOEC, where conditioned CO₂ is superheated, mixed with superheated steam and reformed with preheated air to an H₂-rich gas and CO. The synthesis gas leaving the co-SOEC is cooled and condensed in four stages before entering the FT-reactor.

FT-reactor and upgrading A catalytic conversion of the synthesis gas at high temperatures and pressure is carried out in the FT-reactor. The resulting syncrude is separated into FT-wax, diesel and naphtha and upgraded for final use. The product properties downstream of the separation are given in Appendix A. Unreacted synthesis gas is partially recirculated and fed into the combustion system.

Combustion System The combustion system (CS) comprises three serially connected combustion chambers. Unreacted synthesis gas from the separation

is used as fuel gas. The CS serves as an internal hot utility to heat the cold process streams.

2.2. Methods

The operating point of the co-SOEC influences the stream parameters inlet, outlet temperature and heat capacity flow of the HEN and vice versa; a holistic optimum can only be achieved by coupling operation and design optimization. The optimization performed in this paper is based on the extension of the classical heat exchanger network synthesis (HENS) by Huber et al. [10, 12]. The HENS of Yee & Grossman [13] has been adapted to implement streams with variable temperatures and heat flow capacities. Furthermore, the formulation has been extended to include operating characteristics in the optimization problem. A fundamental assumption for this is that distinct operating points affect only the stream parameters and the objectives. For each operating variable, a piece-wise linear model is created to represent the interaction between the operating point and the stream parameters. For further information regarding the coupled optimization, we refer to [10].

In the case of the PtL-plant, the costs for CO₂ and electricity significantly influence the production costs. Therefore, the multi-criteria optimization problem is solved in

the first instance, considering today’s electricity and CO₂ costs. Based on the resulting non-dominated solutions, the cost parameters are varied to study their impact on PtL-efficiency and production costs. The domain in which the parameters vary is specified, considering future development scenarios with rising and falling prices. In a subsequent step, the objectives are recalculated with modified cost parameters for the given design and operating points of the non-dominated solutions. If objectives are recalculated with different parameters while the variables remain the same, this usually does not lead to optimal results. The choice of parameters affects the solution space of the optimization problem, so optimality cannot be guaranteed. In any case, optimality can be achieved by resolving the optimization problem. However, the objective functions cost parameters we vary do not require re-solving the optimization problems. This remarkably efficient approach is possible because the cost parameters do not directly affect the PtL-efficiency and only linearly affect the production costs. As a result, the non-dominated solutions of the Pareto front are only linearly shifted by the production costs at constant efficiency. This procedure enables us to highly efficiently assess the influence of different price scenarios on the system performance and production costs without performing time-consuming optimizations.

2.2.1. Multi-Criteria Optimization

In this paper, we use the epsilon constraint method to obtain uniformly distributed solutions on the Pareto front. However, the conventional epsilon constraint method is not able to find solutions in overhanging regions of the Pareto front. To overcome this shortcoming, a double-sided epsilon constraint method [12] is used. Therefore, both sides of the Pareto front are constrained to force the objective into a defined domain.

2.2.2. Linearization & Transfer to MILP

Within the adapted HENS, piece-wise linear approximations are used to model all non-linearities. Both piece-wise convex combinations and plane simplices are used to model the multi-dimensional correlations for HEX areas, energy balances and objectives.

To expedite computation, piece-wise linear approximated functions are transformed into mixed integer linear programming (MILP) with a minimal amount of binary variables. One-dimensional, mainly convex curved

functions are converted to MILP without binary variables, while other functions necessitate binary variables. Employing the logarithmic coding approach, as proposed by Vielma and Nemhauser [14], minimizes the number of binary variables.

Additional information on the methods applied regarding the piece-wise linear approximation and the conversion to MILP can be found in [12].

3. Modeling

The modeling of the system is based on steady-state simulations with Aspen HYSIS. The main operating parameter of the PtL-plant is the cell voltage of the co-SOEC. The system was simulated for seven equidistant cell voltages between $U_{\text{cell}}^{\text{min}} = 1.275 \text{ V}$ and $U_{\text{cell}}^{\text{max}} = 1.305 \text{ V}$. The simulation data is used to model the system. Feedstock, power consumption of the co-SOEC, product output, and stream data for the HENS are modeled as a function of cell voltage. The systems’ subcomponents’ size is independent of the cell voltage, resulting in identical system costs. The size of the CS providing the internal heat is also independent of the cell voltage. Only the available amount of FT-offgas is limited depending on the cell voltage.

Detailed information on system modeling can be found in [10]. The parameters used to specify the streams and the heat exchanger network are given in Appendix B.

3.1. Objectives

Multi-objective optimization enables a holistic performance evaluation of the PtL-plant. In this paper, the antagonistic objectives PtL-efficiency and fuel production costs are optimized.

3.1.1. PtL-Efficiency

PtL-efficiency is maximized and described as the ratio of chemically bounded energy in the product \dot{H}_{prod} to electrical energy input P_{el} according to Equation (1).

$$\max \eta_{\text{PtL}} = \frac{\dot{H}_{\text{prod}}}{P_{\text{el}}} = \frac{\sum_v \dot{m}_{\text{prod},v} h_{\text{prod},v}}{P_{\text{sys}} + \sum_j \varepsilon_{\text{hu}} q_{\text{hu},j} + \sum_i \varepsilon_{\text{cu}} q_{\text{cu},i}} \quad (1)$$

The chemically bonded energy downstream of the separation is derived from the sum of the product mass flow rates and the specific enthalpies.

A significant part of the total electrical energy demand P_{el} is the system power P_{sys} . With P_{sys} , the electric demand of the co-SOEC, circulation pumps, valves and control equipment and losses are covered. The two sums in the denominator represent the energy demand of the electrified utilities. A coefficient of performance of $\varepsilon_{cu} = 0.05$ is assumed for the cold utilities. For the hot utilities, ε_{hu} is assumed to be 1.05.

3.1.2. Fuel Production Costs

The fuel production costs c_{prod} are minimized and modeled according to Equation (2) as the ratio of total annual costs TAC to total synthetic fuel output $\sum_v t \dot{m}_{prod,v}$.

$$\min c_{prod} = \frac{TAC}{\sum_v t \dot{m}_{prod,v}} = \frac{CAPEX + OPEX}{\sum_v t \dot{m}_{prod,v}} \quad (2)$$

The capital expenditures $CAPEX$ according to Equation (3) are composed of investment costs for the system C_{sys} and costs for the heat exchanger network according to Yee & Grossmann [13].

$$\begin{aligned} CAPEX = & AF_{inv} \left[\underbrace{C_{sys}}_{\text{investment costs}} + \underbrace{\sum_i \sum_j \sum_k c_{v,hex} \left(\frac{q_{ijk}}{U_{ij} LMTD_{ijk}} \right)^\beta}_{\text{variable HEX stream costs}} \right. \\ & + \underbrace{\sum_i c_{v,hex} \left(\frac{q_{cu,i}}{U_{cu,i} LMTD_{cu,i}} \right)^\beta}_{\text{variable HEX cold utility costs}} \\ & + \underbrace{\sum_j c_{v,hex} \left(\frac{q_{hu,j}}{U_{hu,j} LMTD_{hu,j}} \right)^\beta}_{\text{variable HEX hot utility costs}} \\ & \left. + \underbrace{\sum_i \sum_j \sum_k c_{f,hex} z_{ijk} + \sum_i c_{f,hex} z_{cu,i} + \sum_j c_{f,hex} z_{hu,j}}_{\text{fixed investment costs hex}} \right] \quad (3) \end{aligned}$$

The operating expenditures $OPEX$ according to Equation (4) are feedstock and electricity costs depending on the

annual full load hours t .

$$\begin{aligned} OPEX = & AF_{op} t \left[\underbrace{c_{CO_2} \dot{m}_{CO_2} + c_{H_2O} \dot{m}_{H_2O} + c_{air} \dot{m}_{air}}_{\text{feedstock costs}} \right. \\ & \left. + c_{el} \left(P_{sys} + \sum_j \varepsilon_{uh} q_{uh,j} + \sum_i \varepsilon_{uc} q_{uc,i} \right) \right] \quad (4) \end{aligned}$$

electricity costs

3.2. Cost Parameters

The coupled optimization of the PtL-plant is performed with initial values for electricity and CO₂ costs based on current market conditions. Figure 2 shows the chosen domain of cost parameters. The production of synthetic fuels can only be climate neutral if only CO₂-neutral produced electricity is used. For a location in central Europe and electricity production from wind and solar PV, Janssen et al. [15] suggest a price of $c_{el,base} = 20 \text{ €/}(MW h)$. For the lower electricity price limit $c_{el,min}$, we refer to Sens et al. [16] where in 2050, electricity from PV and wind onshore can be expected to have a levelized cost of electricity (LCOE) of approximately $10 \text{ €/}(MW h)$. We consider this as a best-case scenario for future electricity price developments. The upper limit of $c_{el,max} = 100 \text{ €/}(MW h)$ is derived from the LCOE for wind offshore in 2050 [16].

The price for emitted CO₂ can be levied either with a cap-and-trade system like the Emission Trading System (ETS) or as a carbon tax [17]. Both policies aim to have the government financially penalize greenhouse gas emissions and thus force the polluters to reduce. What CO₂ pricing will look like for synthetic fuels has not yet been defined. In any case, it can be assumed that the end users will bear the costs. In this paper, we use a CO₂ price of $c_{CO_2,base} = 50 \text{ €/t}$ as a base value. This corresponds roughly to the average CO₂ tax in Europe according to the Carbon Pricing Dashboard of The World Bank [18]. A minimum price of $c_{CO_2,min} = 0 \text{ €/t}$ is assumed as an economic best-case scenario. This scenario represents sites with no CO₂ pricing or where special regulations for synthetic fuels have been enacted. As a maximum value, a

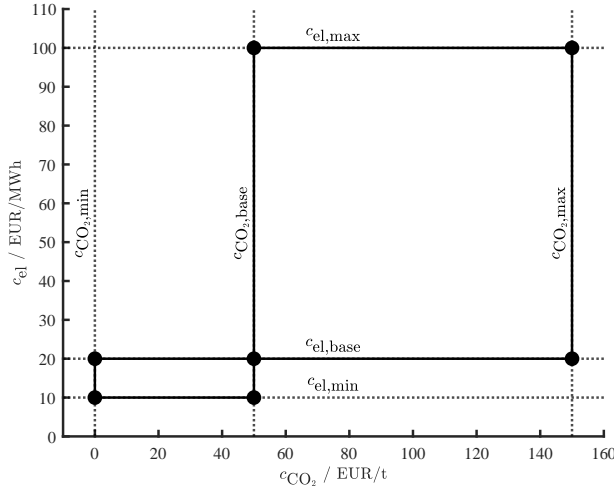


Figure 2: Upper and lower limits of the cost parameters for electricity c_{el} and CO_2 c_{CO_2} .

CO_2 price of $c_{CO_2,min} = 150 \text{ €/t}$ is assumed. This represents a roadmap for realistic price development towards 2050 [19, 20, 21].

3.3. Implementation

The optimization problem was formulated with Yalmip R20210331 [22] and Matlab R2022b [23]. Gurobi 10.0.0 was used as MILP solver [24]. A MIP gap of less than 1% was set as a termination criterion for the optimization. All computations were performed on a 64-core server (AMD EPYC 7702P) with 265 GB of RAM.

All non-linearities are piecewise linearly approximated, analogous to the approach from Huber et al. [10]. A root-mean-square error (RMSE) of less than 1% is set as a termination criterion for the refinement of the approximations.

All cost parameters are given in Appendix C.

4. Results

The non-dominated solutions of the antagonistic objectives are illustrated as a Pareto front in Figure 3. The color coding represents the cell voltage as the critical operating parameter. The slight scattering of the Pareto front at low production costs results from the solver time out and the optimality gap of the solution. There were no solutions

found for the gaps around high production costs within the defined solver time. The stream plots at the corner points of the Pareto front and the characteristic values such as number the of heat exchangers, power of the utilities and the costs can be obtained from [10].

An essential aspect of the Pareto front is that the production costs increase with decreasing cell voltage. Further, the shape of the Pareto front allows us to derive the impact of design and operating parameters. At the highest cell voltage of $U_{cell} = 1.305 \text{ V}$, the PtL-efficiency remains almost unchanged between 57.67% and 58.35%. The production costs, however, vary from 1.83 €/kg to 2.06 €/kg. This indicates that design parameters significantly influence production costs but only barely the efficiency in this region. Conversely, at the upper production cost range, the influence of the cell voltage dominates. The production costs remain almost constant while the PtL-efficiency increases significantly.

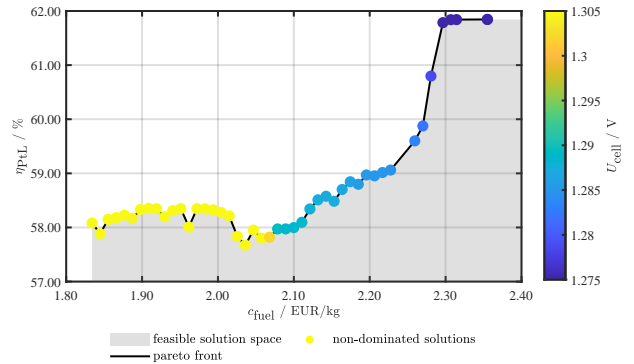


Figure 3: Non-dominated solutions and Pareto front of the coupled optimization. The color coding represents the cell voltage as the main operating parameter.

Price changes are analyzed based on the non-dominated solutions optimized with initial cost parameters. Production costs are recalculated for each solution at constant PtL-efficiencies. This is feasible because the cost parameters for CO_2 and electricity occur as linear terms only in the objective function of the production costs and not in that of the PtL-efficiency; see Equation (2) and (4), respectively. Thus, only the production costs change depending on the cost parameters, while the PtL-efficiency remains unchanged. We quantify the impact of the cost parameters with the help of the parameter sensitivity de-

defined by Equation (5) and (6).

$$\nabla c_{el} = AF_{op} \frac{\left[P_{sys} + \left(\sum_j \varepsilon_{uh,j} q_{uh,j} + \sum_i \varepsilon_{uc} q_{uc,i} \right) \right]}{\sum_v \dot{m}_{prod,v}} \quad (5)$$

$$\nabla c_{CO_2} = AF_{op} \frac{\dot{m}_{CO_2}}{\sum_v \dot{m}_{prod,v}} \quad (6)$$

Figure 4 on the top shows the sensitivities to electricity price changes. With an annualization factor of $AF_{op} = 1$, ∇c_{el} can be interpreted as energy consumption to produce 1 kg of synthetic fuel, respectively FT-wax, diesel and naphtha. Fasihi et al. obtained a slightly higher value of 21.98 kWh/kg for a similar PtL-plant with an ambient air scrubber, reverse water gas shift reaction (RWGS) and alkaline electrolysis cell [25]. In our case, PtL-efficiency strongly correlates with the sensitivity. Higher efficiencies are, therefore, less susceptible to price changes.

The sensitivities to CO_2 price changes are shown in Figure 4 on the bottom. They can be interpreted as the utilized amount of CO_2 per kg of synthetic fuel produced. The process presented by Fasani et al. [25] requires 3.20 kg/kg. In this case, the sensitivity correlates less strongly with the efficiency but instead much more with the cell voltage. Therefore, plant designs with low cell voltages are less susceptible to price changes.

Based on the sensitivities, we calculated the production costs for each non-dominated solution as function of the electricity and CO_2 prices. Figure 5 shows the highest and lowest production costs. The minimum and maximum production costs are shown as a function of electricity prices on the left and CO_2 prices on the right. The horizontal lines show the current cost parameters $c_{el,base}$ and $c_{CO_2,base}$ from Figure 2. The minimum and maximum production costs are shown for both cost parameters on the right side of Figure 5. All non-dominated solutions are between these two planes. In this context, the sensitivities can be interpreted as slopes of the limiting lines, respectively, planes. Accordingly, the higher the sensitivity, the more sensitive the solution reacts to price changes. It can be concluded from the plane slopes that the influence of the electricity price on the production costs is about five times larger than that of the CO_2 price.

The price changes affect the shape of the Pareto front depending on the efficiency. On the top of Figure 6, three Pareto fronts for minimum, initial and maximum electric-

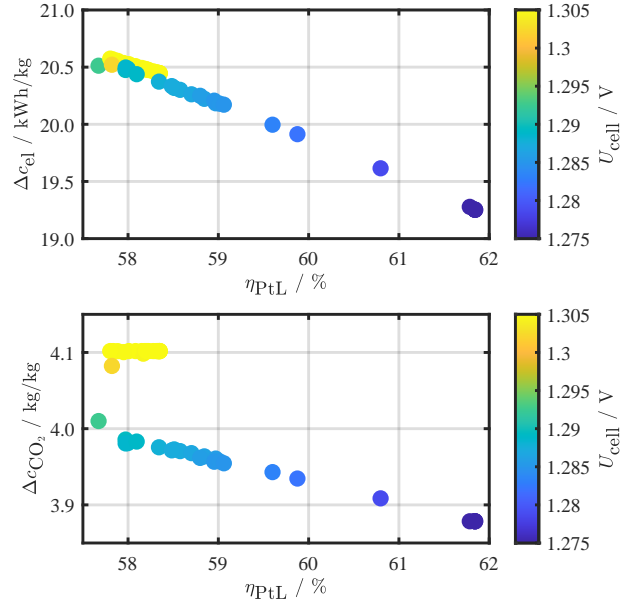


Figure 4: Calculated sensitivities for electricity and CO_2 price changes as a function of PtL-efficiency.

ity prices are shown. Electricity prices have a substantial effect on production costs. When electricity costs are high, it is noticeable that the Pareto front forms a pocket in the efficiency range from 59.0 % to 61.8 %. If higher electricity costs are expected, selecting a plant design with these parameters should be avoided since lower production costs can be expected at higher and lower efficiencies. The Pareto fronts for different CO_2 prices in Figure 6 on the bottom do not create pockets. It is noticeable that the influence on the production costs is significantly lower.

Figure 7 shows the collective impact of price changes. For each extreme value, a Pareto front is shown. It should be noted that the lines for $c_{CO_2,min}$ and $c_{el,min}$ overlap almost completely. If the electricity price is reduced to 10 €/MW and the CO_2 price is dropped to 0, synthetic fuels can be produced in the 1.42 €/kg to 1.97 €/kg range. Compared to the current market price for gasoline of about 0.5 €/kg, the large-scale introduction of synthetic fuels will be an economic challenge [26]. At the highest electricity and CO_2 prices of 100 €/MW and 150 €/t, the production costs range from 3.88 €/kg to 4.28 €/kg. Whether synthetic fuels will prevail at this price level is questionable.

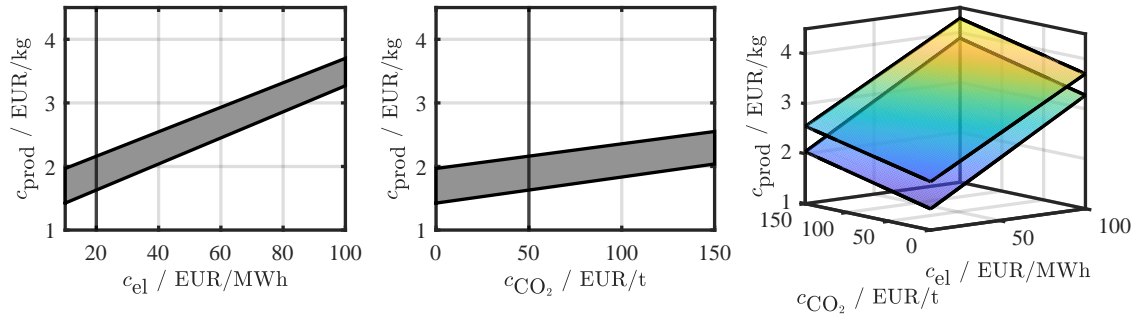


Figure 5: Upper and lower production costs as a function of electricity and CO₂ price. Left: Isolated impact of electricity price. Middle: Isolated impact of the CO₂ price. Right: Combined impact.

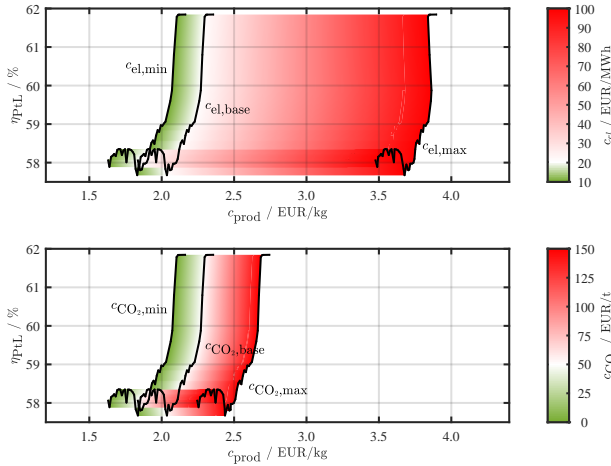


Figure 6: Pareto fronts for changing electricity prices (top) and CO₂ prices (bottom). The color gradient represents the shift of the Pareto front due to price changes.

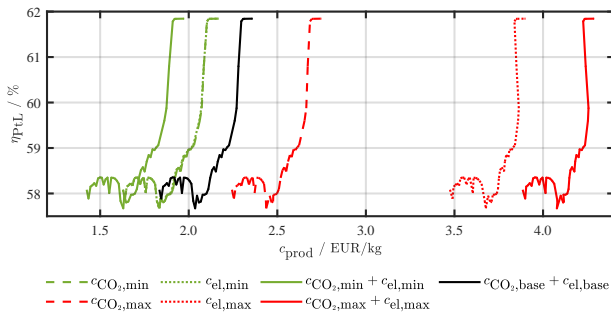


Figure 7: Pareto fronts for the extreme values of the cost parameters: Initial costs (black), cost reduction (green), cost increase (red).

5. Conclusion

In this paper, we investigated the impact of changing electricity and CO₂ prices on the production costs of synthetic fuels. A novel 1 MW PtL-plant was considered as a use case. The main components were modeled and the cell voltage of the co-SOEC was optimized as a crucial operating parameter coupled with the heat exchanger network and the internal heat supply as design parameters. A formulation for PtL-efficiency and production cost was presented as objective functions. Based on the optimization results, the sensitivities for electricity and CO₂ price changes were calculated and their correlation with the design and operational parameters was discussed. A comprehensive cost analysis was performed with defined scenarios for decreasing and increasing cost parameters.

Our results show that the non-dominated solutions of the Pareto front in the low-efficiency area depend more on the design parameters than on the cell voltage of the co-SOEC as the operating parameter. On the other hand, a distinct dependence on the cell voltage can be seen in the high-efficiency area. Current electricity and CO₂ prices results in production costs in the range of 1.83–2.36 €/kg and a PtL-efficiency of 57.67–61.84 %. Further, we were able to show that the influence of the electricity price is about five times larger than that of the CO₂ price. The sensitivity of the electricity price correlates strongly inversely with the efficiency. This implies that higher efficiencies are less affected by price increases. Substantial price increases lead to pockets in the Pareto front, which may preclude specific design and operating areas. A further key outcome is that our results allow us to estimate the ex-

pected production costs depending on price changes. In the economic best-case scenario, production costs can be reduced to the range of 1.42–1.97 €/kg. In the worst-case scenario, production costs increase up to 3.88–4.28 €/kg.

With this paper, we provide an overview of current production costs and the influence of design and operating parameters on future cost developments. A central and, above all, necessary basis for decision-making has been developed with this paper. It enables the decision-makers to evaluate the design and its consequences for sustainable synthetic fuel production. With this paper, we promote the efficient and cost-effective production of synthetic fuels and contribute significantly to a climate-neutral and sustainable future.

References

- [1] International Energy Agency, CO2 Emissions in 2022, Technical Report, 2022. URL: <https://www.iea.org/reports/co2-emissions-in-2022>.
- [2] International Energy Agency, Global CO2 emissions from transport by sub-sector in the Net Zero Scenario, Technical Report, 2022. URL: <https://www.iea.org/energy-system/transport>.
- [3] F. Ueckerdt, C. Bauer, A. Dirnaichner, J. Everall, R. Sacchi, G. Luderer, Potential and risks of hydrogen-based e-fuels in climate change mitigation, *Nature Climate Change* 11 (2021) 384–393. doi:10.1038/s41558-021-01032-7, number: 5 Publisher: Nature Publishing Group.
- [4] S. Pratschner, M. Hammerschmid, S. Müller, F. Winter, Evaluation of CO2 sources for Power-to-Liquid plants producing Fischer-Tropsch products, *Journal of CO2 Utilization* 72 (2023) 102508. doi:10.1016/j.jcou.2023.102508.
- [5] eFuel Alliance e.V., eFuel Produktionskarte, 2023. URL: <https://www.efuel-alliance.eu/de/efuels/efuel-produktionskarte>.
- [6] Fraunhofer IEE, Global PtX Atlas 1.2.1 (Januar 2023), 2023. URL: <https://maps.iee.fraunhofer.de/ptx-atlas/>.
- [7] Siemens energy, Haru Oni: Base camp of the future, 2023. URL: <https://www.siemens-energy.com/global/en/news/magazine/2022/haru-oni.html>.
- [8] T. Ngan Do, C. You, J. Kim, A CO2 utilization framework for liquid fuels and chemical production: techno-economic and environmental analysis, *Energy & Environmental Science* 15 (2022) 169–184. doi:10.1039/D1EE01444G, publisher: Royal Society of Chemistry.
- [9] M. Mahrach, G. Miranda, C. León, E. Segredo, Comparison between Single and Multi-Objective Evolutionary Algorithms to Solve the Knapsack Problem and the Travelling Salesman Problem, *Mathematics* 8 (2020) 2018. doi:10.3390/math812018.
- [10] D. Huber, F. Birkelbach, R. Hofmann, Unlocking the Potential of Synthetic Fuel Production: Coupled Optimization of Heat Exchanger Network and Operating Parameters of a 1 MW Power-to-Liquid Plant, *Chemical Engineering Science* (2023) 119506. doi:10.1016/j.ces.2023.119506.
- [11] D. Huber, K. Werding, F. Birkelbach, R. Hofmann, Highly efficient heat integration of a power-to-liquid process using MILP, in: 36th International Conference on Efficiency, Cost, Optimization, Simulation and Environmental Impact of Energy Systems (ECOS 2023), volume I, part A-I, ULPGC, Las Palmas De Gran Canaria, Spain, 2023, pp. 1513–1523.
- [12] D. Huber, F. Birkelbach, R. Hofmann, HENS Unchained: MILP Implementation of Multi-Stage Utilities with Stream Splits, Variable Temperatures and Flow Capacities, *Energies* 16 (2023) 4732. doi:10.3390/en16124732.
- [13] T. F. Yee, I. E. Grossmann, Simultaneous optimization models for heat integration—II. Heat exchanger network synthesis, *Computers & Chemical Engineering* 14 (1990) 1165–1184. doi:10.1016/0098-1354(90)85010-8.
- [14] J. P. Vielma, G. L. Nemhauser, Modeling disjunctive constraints with a logarithmic number of binary

- variables and constraints, *Mathematical Programming* 128 (2011) 49–72. doi:10.1007/s10107-009-0295-4.
- [15] J. Janssen, M. Weeda, R. J. Detz, B. van der Zwaan, Country-specific cost projections for renewable hydrogen production through off-grid electricity systems, *Applied Energy* 309 (2022) 118398. doi:10.1016/j.apenergy.2021.118398.
- [16] L. Sens, U. Neuling, M. Kaltschmitt, Capital expenditure and levelized cost of electricity of photovoltaic plants and wind turbines – Development by 2050, *Renewable Energy* 185 (2022) 525–537. doi:10.1016/j.renene.2021.12.042.
- [17] P. K. Kruse-Andersen, P. B. Sørensen, Optimal carbon taxation in EU frontrunner countries: coordinating with the EU ETS and addressing leakage, *Climate Policy* (2022) 1–13. doi:10.1080/14693062.2022.2145259.
- [18] The World Bank, Carbon Pricing Dashboard, 2023. URL: https://carbonpricingdashboard.worldbank.org/map_data.
- [19] BloombergNEF, Carbon Offset Prices Could Increase Fifty-Fold by 2050, 2023. URL: <https://about.bnef.com/blog/carbon-offset-prices-could-increase-fifty-fold-by-2050/>.
- [20] Essential, expensive and evolving: The outlook for carbon credits and offsets, Technical Report, EY Net Zero Centre, Sydney, 2022.
- [21] GHG Market Sentiment Survey 2022, Technical Report, IETA, 2022. URL: <https://www.ieta.org/resources/Documents/IETA%20GHG%20Market%20Sentiment%20Survey%20Report%202022.pdf>.
- [22] J. Löfberg, A toolbox for modeling and optimization in MATLAB, Proceedings of the CACSD Conference (2004) 289. doi:10.1109/CACSD.2004.1393890.
- [23] The MathWorks Inc., MATLAB version: 9.13.0 (R2022b), 2022. URL: <https://www.mathworks.com>.
- [24] Gurobi Optimization, LLC, Gurobi Optimizer Reference Manual, 2023. URL: <https://www.gurobi.com>.
- [25] M. Fasihi, D. Bogdanov, C. Breyer, Techno-Economic Assessment of Power-to-Liquids (PtL) Fuels Production and Global Trading Based on Hybrid PV-Wind Power Plants, *Energy Procedia* 99 (2016) 243–268. doi:10.1016/j.egypro.2016.10.115.
- [26] U.S. Energy Information Administration, U.S. Total Gasoline Wholesale/Resale Price by Refiners (Dollars per Gallon), 2023. URL: <https://www.eia.gov/petroleum/data.php>.
- [27] S. Adelung, Global sensitivity and uncertainty analysis of a Fischer-Tropsch based Power-to-Liquid process, *Journal of CO2 Utilization* 65 (2022) 102171. doi:10.1016/j.jcou.2022.102171.
- [28] G. Herz, C. Rix, E. Jacobasch, N. Müller, E. Reichelt, M. Jahn, A. Michaelis, Economic assessment of Power-to-Liquid processes – Influence of electrolysis technology and operating conditions, *Applied Energy* 292 (2021) 116655. doi:10.1016/j.apenergy.2021.116655.
- [29] V. Dieterich, A. Buttler, A. Hanel, H. Spliethoff, S. Fendt, Power-to-liquid via synthesis of methanol, DME or Fischer-Tropsch-fuels: a review, *Energy & Environmental Science* 13 (2020) 3207–3252. doi:10.1039/D0EE01187H.
- [30] DACE price booklet: cost information for estimation and comparison, edition 35 ed., DACE Cost and Value, Nijkerk, 2021. OCLC: 1303572720.
- [31] EurEau, Europe’s Water in Figures: An overview of the European drinking water and waste water sectors, 2021. URL: <https://www.eureau.org/resources/publications/eureau-publications/5824-europe-s-water-in-figures-2021/file>.

Statements and Declarations

Funding

This research was funded by the Austrian Research Promotion Agency (FFG) under grant number 884340 and TU Wien Bibliothek through its Open Access Funding Programme.

Competing Interests

The authors have no relevant financial or non-financial interests to disclose.

Authors Contributions

The method presented in this paper was developed by David Huber. Testing and evaluation was done by David Huber. The conceptualization of the paper was done by all authors. The first draft was written by David Huber. All authors contributed to the revision of the initial draft. Funding and supervision was done by René Hofmann. All authors read and approved the final manuscript.

Appendix A. Product Properties

Table A.1 lists the chemical and physical product parameters. These are invariant for the system regardless of the cell voltage.

Table A.1: Chemical and physical product properties at 40 °C and 101 324.97 Pa downstream the upgrading. Adapted from [10].

ν	product	$h_{\text{prod}} / \text{MJ/kg}$	$\rho_{\text{prod}} / \text{kg/m}^3$	$\mu_{\text{prod}} / \text{mPa/s}$
1	FT-wax	43.887	797.73	6.7477
2	diesel	44.345	748.81	1.5983
3	naphtha	44.676	516.17	0.5893

Appendix B. Stream Data

Table B.2 provides the stream parameters or their bounds. Values without brackets are independent of the cell voltage constant. Values in square brackets are bounds of stream parameters dependent on cell voltage. The heat transfer coefficients are $U = 0.5 \text{ kW}/(\text{m}^2 \text{ K})$ for all streams.

The HEN problem has been modeled with $N_{\text{st}} = 3$ stages for the heat exchange. The minimum temperature difference of $\Delta T_{\text{min}} = 1 \text{ K}$ must not be exceeded.

Table B.2: Stream data with limits for inlet, outlet temperature and flow capacity. Adapted from [10].

Stream	$T^{\text{in}} / ^\circ\text{C}$	$T^{\text{out}} / ^\circ\text{C}$	$F / \text{kW/K}$
H1	40.0	35.0	[1.71, 2.16]
H2	[127.9, 131.1]	[34.0, 35.0]	[0.09, 0.12]
H3	[169.8, 174.1]	[34.0, 35.0]	[0.09, 0.12]
H4	210.0	190.0	[0.27, 0.28]
H5	190.0	120.0	[0.56, 0.58]
H6	120.0	30.0	[0.48, 0.50]
H7	[45.4, 57.0]	31.0	[2.35, 2.95]
H8	138.9	137.9	[59.60, 94.40]
H9	[805.2, 825.5]	[34.0, 35.0]	[0.10, 0.13]
H10	[49.5, 50.7]	[34.0, 35.0]	[0.65, 0.88]
H11	101.8	30.0	[0.51, 0.64]
H12	190.0	188.0	[76.88, 80.45]
C1	[318.0, 319.2]	[825.0, 870.5]	[0.14, 0.18]
C2	116.9	124.2	[20.02, 25.12]
C3	[57.3, 58.8]	825.0	[0.25, 0.33]
C4	137.9	139.9	[105.77, 142.64]
C5	138.9	[426.6, 449.4]	[0.10, 0.11]
C6	35.0	[115.9, 145.4]	[0.05, 0.06]
C7	20.3	[189.5, 199.6]	[0.15, 0.21]
CS1	900.0	[100, 890]	[59.60, 94.40]
CS2	900.0	[100, 890]	[0.10, 0.13]
CS3	900.0	[100, 890]	[0.65, 0.88]

Appendix C. Cost Parameters

Table C.3 lists the cost parameters and their sources. The investment costs are depreciated linearly over a period of 20 years. Thus, the annual depreciation factor is $AF_{\text{inv}} = 1/20y$. The depreciation factor for the operating costs is assumed to be $AF_{\text{op}} = 1/y$. Analogous to [27, 28, 29], $t = 8000 \text{ h/y}$ full load operating hours per year are assumed.

Nomenclature

Acronyms

CAPEX	annual capital expenses
CS	combustion system

Table C.3: Cost parameters and their source. Adapted from [10].

cost share	value	comment / source
β	0.8	
$c_{f,\text{hex}}$	1013.6 €/y	AISI 316, interpolated from [30]
$c_{v,\text{hex}}$	61.8 €/(m ² β y)	
C_{sys}	10 000 000 €	project internal estimation & [28]
$c_{\text{H}_2\text{O}}$	3.54 €/t	mean for Europe [31]
$c_{\text{CO}_2,\text{base}}$	50 €/t	average CO ₂ tax in Europe [18]
c_{air}	0 €/t	ambient air is free of charge
$c_{\text{el},\text{base}}$	20 €/(MW h)	at a projected plant location in Europe [15]

ETS	emission trading system
FT	fischer-tropsch
HEN	heat exchanger network
HENS	heat exchanger network synthesis
HEX	heat exchanger
IFE	Innovation Flüssige Energie, eng.: Innovation Liquid Energy
LCOP	levelized cost of product
LMTD	logarithmic mean temperature difference
MILP	mixed-integer linear programming
MIP	mixed-integer programming
MOO	multi objective optimization
OPEX	operational expenditures
PtL	power-to-liquid
PV	photovoltaics
RMSE	root-mean-square error
RWGS	reverse water gas shift
SOEC	solid oxide electrolysis cell

Superscripts

in	inlet
max	maximum

min minimum

out outlet

Subscripts

cu	cold utility
el	electric
hex	heat exchanger
hu	hot utility
prod	production
i	hot stream
j	cold stream
k	stage

Variables

β	cost exponent	
ΔT_{min}	minimum temperature difference	K
\dot{H}	chemically bounded energy in products	FT-kW
\dot{m}	mass flow	kg/h
η_{PtL}	PtL-efficiency	%
$CAPEX$	capital expenditures	€/y
$CAPEX$	operating expenditures	€/y
$LMTD$	logarithmic mean temperature difference	K
TAC	total annual costs	€/y
μ	dynamic viscosity	mPa/s
ρ	density	kg m ³
ε	coefficient of performance	
a	depreciation period	y
AF_{inv}	investment annualization factor	1/y
AF_{op}	operational annualization factor	

c_{el}	electricity costs	€/ (MW h)
$c_{f,hex}$	step-fixed HEX costs	€/y
c_{prod}	product costs	€/kg
C_{sys}	investment costs	€
$c_{v,hex}$	variable HEX costs	€/ (m ^{2β} y)
c_f	feedstock costs	€/t
F	flow capacity	kW/K
h_{prod}	specific enthalpy of the product	MJ/kg
N_{st}	number of stages	
P_{el}	total electrical energy demand	kW
P_{sys}	electrical energy demand w/o utilities	kW
q	heat flow	kW
T	temperature	°C
t	annual full load hours	h/y
U	overall heat transfer coefficient	kW/(m ² K)
U_{cell}	cell voltage	V
z	binary variable for existence of HEX	